Nickel self-diffusion in a liquid and undercooled NiSi alloy

F. Demmel, L. Hennet, S. Brassamin, D. Neuville, J. Kozaily, M. Koza

Nickel self-diffusion in a liquid and undercooled NiSi alloy

F. Demmel,[1,*] L. Hennet,[2] S. Brassamin,[2] D. R. Neuville,[3] J. Kozaily,[4] and M. M. Koza[5]
[1]*ISIS Facility, Rutherford Appleton Laboratory, Didcot, OX11 0QX, United Kingdom*
[2]*CNRS-CEMHTI, University of Orléans, 45071 Orleans, France*
[3]*IPGP, Sorbonne Paris Cité, 75005 Paris, France*
[4]*Rafik Hariri University, P.O. Box 10, Damour-Chouf 2010, Lebanon*
[5]*Institut Laue-Langevin, 71 avenue des Martyrs, CS 20156, 38042 Grenoble cedex 9, France*
(Received 29 January 2016; revised manuscript received 23 June 2016; published 18 July 2016)

The nickel self-diffusion coefficient was measured in a $Ni_{75}Si_{25}$ alloy in the liquid and undercooled state by quasielastic neutron scattering. The undercooled state was achieved by applying aerodynamic levitation. That containerless technique allowed an undercooling of $\Delta T \approx 90$ K over 4 h of measurement time. The temperature dependence of the derived diffusion coefficients follows an Arrhenius-type behavior. The activation energy for the diffusion process is about 10% larger than in pure nickel and is probably the reason for the slower self-diffusion coefficient compared to pure Ni. With increasing Si content more covalent bonding is formed, which might be the origin for the reduced mobility. Molecular dynamics simulations predicted a change in dynamics from an Arrhenius-type behavior to a power-law for temperatures as high as twice the glass transition temperature. Our data are compatible with a power-law behavior for the Ni self-diffusion.

DOI: 10.1103/PhysRevB.94.014206

I. INTRODUCTION

Understanding the dynamics of liquid metals and alloys is relevant for technological applications like solidification and welding. During processing nearly all metals undergo a step in the liquid phase. The liquid state is limited by a first-order transition to a crystalline state, and if a crystalline state is reached a dramatic change in long-range order occurs manifesting the first-order phase transition. However, if crystallization can be avoided the liquid can be undercooled and eventually the material morphs into a glass [1] with potential new properties.

Nickel-based alloys cover a wide field of applications, for example, when high strength at high temperature is needed. To achieve these requirements other elements like aluminium and silicon are added to nickel. For a further optimization of the materials, a deeper understanding of the relevant processes toward solidification is necessary [2]. From the application point of view within the nickel-based alloys NiSi compounds might have potential as high-temperature and oxidation-resistant alloys, and NiSi nanowires have been proposed as electrical contacts in electronic devices [3]. Single crystal superalloys depend on directional solidification and hence on the particle mobility for growing grains [4]. The diffusion coefficient is an important parameter to describe solidification at the liquid-solid interface. However, there is a lack of experimental data for self-diffusion coefficients due to experimental difficulties related to high temperatures or to measure within the metastable state at all. An experimental method to measure self-diffusion coefficients, not influenced by convection in the liquid, is quasielastic neutron scattering (QENS), because QENS probes the movement of the particles on a picosecond timescale and hence is not sensitive to the much slower convective movements.

The binary solid NiSi compound shows a range of phases depending on the composition [5] and has recently been assessed by a first-principles study [6]. Which of these phases is chosen upon cooling depends on composition but also on process parameters like cooling rate and melt undercooling [7]. For the NiSi melt a nonideal mixing behavior was shown [8]. The molar volume decreases at first with rising Si concentration hinting to strong interactions between the particles. A consequence of this mixing effect might be the tendency for an increased glass forming ability with increasing Si content as observed in MD simulations [8].

A previous structural study on liquid NiSi melt compositions came to the conclusion that this binary melt does not show any compound formation and might even be regarded as a hard spheres liquid in a first approximation [9]. The derived partial structure factors are apparently similar to the ones from the pure Ni and Si liquids. However, a later neutron diffraction experiment on silicon-rich compositions with isotope substitution revealed an influence on the atomic structure due to silicon's tendency to covalent bonding in the $Ni_{50}Si_{50}$ melt [10]. The interplay of structure and dynamics was observed in a QENS study on the Ni self-diffusion of the silicon-rich compounds, which demonstrated a factor five faster Ni diffusion compared to pure liquid nickel [11,12]. This experiment was performed by a levitation technique in the 200 K undercooled state and crossing the liquidus temperature did not indicate any change in dynamics. That higher Ni mobility might be related to a more open structure of molten silicon compared to the hard sphere-like structure of molten nickel, evidenced by only six nearest neighbors in the liquid state of the silicon-rich melt [13].

On the nickel-rich side of the phase diagram surface tension measurements have been performed for a Ni-5wt%Si alloy in the liquid and about 200 K undercooled state. The derived viscosity and diffusion coefficients have been described by an Arrhenius law across the whole temperature range [14]. Classical MD-simulations have been performed on Ni-rich compositions and no experiments on the microscopic

*franz.demmel@stfc.ac.uk

dynamics, as far as we know [8,15]. The simulations studied the structure and dynamics of NiSi alloys with up to 25 at% Si content. The glass-forming ability increased with the silicon content. The derived self-diffusion coefficients showed with decreasing temperature strong deviations from Arrhenius behavior. The change in dynamics toward a power-law behavior of the self-diffusion coefficient occurs above the melting point and marks the onset of slowing down in dynamics toward the glass transition. Similarly, for the viscosity a non-Arrhenius temperature dependence was found. The product of viscosity and self-diffusion shows a distinct change with temperature deep in the liquid state and evidences a change in dynamics above the melting temperature. Changes in the dynamics above the melting temperature in liquid monatomic metals have been observed for rubidium, lead, and aluminium [16–18]. These metals are not bulk glass formers; however, the dynamics on next-neighbor distances changes distinctly for all three metals at a temperature of about $1.3–1.5T_{\mathrm{melting}}$. That change in microscopic dynamics was related to a more viscous behavior in the liquid state toward freezing or the glass transition. It was suggested that deep in the equilibrium liquid state the slowing down of the structural relaxation toward solidification begins.

Here we want to examine whether $Ni_{75}Si_{25}$ shows the predicted change in dynamics of the self-diffusion process. To this end we present an investigation on the self-diffusion of Ni in a $Ni_{75}Si_{25}$ alloy. Through QENS and applying a gas-jet levitation technique the dynamics was measured in the liquid and about 90 K undercooled state.

II. EXPERIMENTAL DETAILS

Aerodynamic levitation is a simple way to suspend samples, which can be heated independently with lasers. This technique was used successfully in neutron and synchrotron scattering experiments [19,20]. The basic idea is to circulate levitation gas (pure argon in our case) through a nozzle onto the sample from below in order to counteract the gravity and lift it by a few hundred microns inside the nozzle. More details can be found in Refs. [21,22]. Recently, the setup was adapted for inelastic neutron-scattering experiments measurements with an aluminium nozzle [23]. The argon gas flow used during the experiment was fixed to 0.7 l/min. When the sample levitates, it is heated to the desired temperature by means of two 125 W CO_2 lasers operating at 10.6 μm wavelength. The primary laser beam is focused from above by a concave mirror onto the sample with a final beam diameter of 2 mm. The second laser beam from below is mainly used for temperature homogeneity purposes. In order to measure the temperature of the levitated sample with a good precision, two pyrometers are installed working at two wavelengths (0.85 and 0.9 μm). In optimizing the compactness of the setup, one is placed outside the chamber and measures the sample luminescense through a silica window. The second pyrometer, placed inside the chamber, has the advantage to avoid window corrections and was finally used for the temperature measurement.

The $Ni_{75}Si_{25}$ spherical samples were made from weighed amounts of pure nickel and silicon and then melted in the levitator to spherical shape and homogeneous alloys. The cold time of flight IN6 spectrometer at the ILL, France, was operated with an incoming energy $E_i = 3.12$ meV. The chosen incoming wavelength $\lambda_i = 5.12$ Å is above the Bragg cutoff of aluminium. The maximum momentum transfer within that setup of the instrument was 2.0 Å^{-1}. The NiSi sphere had a weight of 75.2 mg, which was reduced after 12 h of heating by a maximum of 1.5 mg and had a diameter of about 2.7 mm. In NiSi only Ni scatters neutrons incoherently. The incoherent neutron cross section of Ni is 5.2 b and the coherent is 13.3 b, whereas the incoherent cross section of silicon is practically zero and the coherent one is 2.163 b [24]. Hence, the neutron-scattering experiment at small wave vectors will observe the self-dynamics of nickel atoms. Toward larger Q-vectors more and more coherent contributions will add to the signal. The first peak of the total structure factor of liquid Ni is at $Q \approx 3.1\ \text{Å}^{-1}$ [25,26] and liquid NiSi shows the first peak at $Q \approx 3.0\ \text{Å}^{-1}$ [9,10] for a wide range of compositions. The melting point of $Ni_{75}Si_{25}$ was deduced from the phase diagram as $T_m = 1513$ K [5]. Several runs were performed at four different temperatures: 1920, 1800, 1535, and 1420 K. According to Wien's law the temperature was calibrated with the measured freezing curves and using the equation: $1/T_{\mathrm{act}} - 1/T_{\mathrm{pyro}} = \text{constant}$, where T_{act} is the actual temperature, T_{pyro} the pyrometer reading, and the constant includes the unknown emissivity of the sample. It is assumed here that the emissivity of the sample remains constant. The constant is derived by comparing the known melting point to the melting plateau observed during the heating stage or the recalescence temperature derived from the freezing curves (see Fig. 1) and then the actual temperature can be deduced. The temperatures have been averaged over the run times. The temperature uncertainty, mainly reasoned by drifts during the measurements was about $\pm 25K$. In Fig. 1 we show two freezing curves taken at the end of two measurements. Both curves demonstrate that the alloy can be undercooled up to 250 K for a short time. It can be noted that the run with the lower temperature ($T \approx 1420$ K) was performed in the undercooled state by about 100 K.

Inelastic spectra were recorded for about 3–4 h per temperature [27]. In addition, a background was taken with the empty levitator and argon-gas-filled sample chamber. A measurement

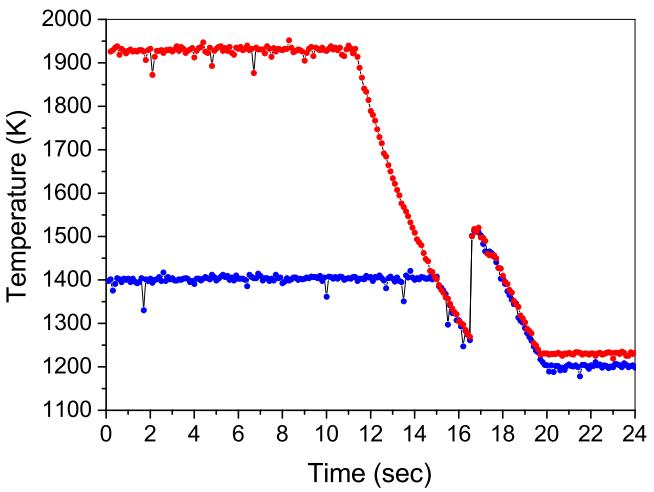

FIG. 1. Freezing curves of two runs at the end of the measurement that demonstrate that one run was performed in the undercooled state.

with a vanadium sphere served for detector efficiency corrections and to determine the energy resolution. The measured energy resolution can be described by a Gaussian function with a full width at half maximum FWHM = 0.077 meV. The measured spectra were monitor normalized, corrected for detector efficiency including the energy efficiency changes of the Helium detectors, and then the measured background has been subtracted. After conversion from time of flight into energy transfer a constant energy binning ($\Delta E = 0.01$ meV) was applied and the spectra were sorted for constant Q values with a Q bin size of $\Delta Q = 0.1$ Å^{-1}. All these steps have been performed with the Lamp-software [28].

Self-diffusion on long time and length scales can be described with the diffusion equation for the density correlation function of a tagged particle. The spatial and time Fourier transformed solution of the diffusion equation is a single Lorentzian with a Q-dependent half width at half maximum (HWHM) $\Gamma_{1/2}(Q)$ [29]:

$$S^s(Q,\omega) = \frac{1}{\pi}\frac{\Gamma_{1/2}(Q)}{(\hbar\omega)^2 + \Gamma_{1/2}(Q)^2}. \quad (1)$$

At small Q vectors, in the hydrodynamic limit ($Q \to 0$), a Lorentzian is the exact line shape for the diffusion behavior and $\Gamma_{1/2}(Q) = \hbar D Q^2$. The proportionality constant D is the self-diffusion coefficient for translational diffusion on long distances. To extract the line width a fit with a single Lorentzian function convoluted with the resolution function was applied. Included into the fit was a linear sloping background, taking care of not-corrected coherent contributions and potential multiple scattering, which are much broader in this wave-vector range compared to the Ni-diffusion signal. In Fig. 2 some spectra including fits with the Lorentzian model are shown. The good fit and the statistics of the data do not recommend the use of a more sophisticated model. In the spectrum for $Q = 0.6$ Å^{-1} [Fig. 2(a)] the empty levitator measurement has been included, which is then subtracted from the sample measurement. A normalized spectrum from the vanadium sphere (dashed line) demonstrates the energy resolution of the spectrometer with our sample size.

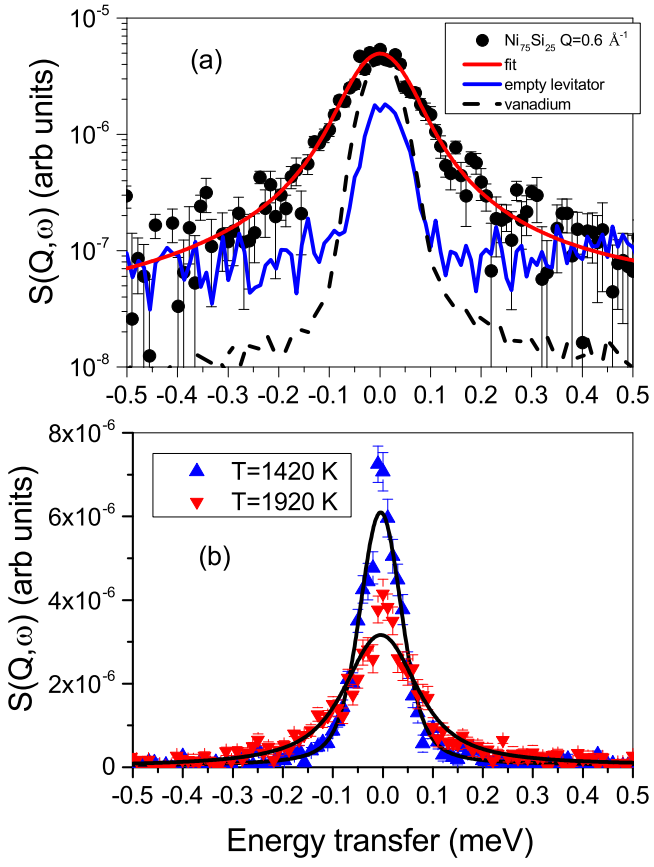

FIG. 2. Plot (a) displays a spectrum at $Q = 0.6$ Å^{-1} for a temperature of $T = 1535$ K and includes the empty levitator measurement (line) and one run with the vanadium sphere (dashed line) on a logarithmic scale. Plot (b) shows 2 spectra at $Q = 0.5$ Å^{-1} for $T = 1420$ K and 1920 K. The lines depict the fit with a Lorentzian curve.

III. RESULTS AND DISCUSSION

In Fig. 2(b) spectra at a wave vector $Q = 0.5$ Å^{-1} are shown for the highest and lowest temperatures. For all temperatures the fit with a single Lorentzian function is sufficient and does not indicate a change in line shape. From the Lorentzian fits we deduced the HWHMs, which are presented in Fig. 3. Note the smallest line width was about 20% of the resolution width. Included in the figure are fits with $\Gamma_{1/2}(Q) = \hbar D Q^2$, which describe the broadening of the spectra quite well in the considered wave vector range and hence allow us to derive the self-diffusion coefficient of nickel. The fit with the diffusion law was applied to a Q range from 0.3 to 0.9 Å^{-1}. Also, the data from the undercooled measurement can be modeled with the DQ^2 diffusion law.

The derived diffusion coefficients are presented in Fig. 4 on a logarithmic scale against the inverse temperature. Included in the figure are values for pure Ni in the liquid and undercooled state [12]. The values between $Ni_{75}Si_{25}$ and liquid Ni are rather similar. In contrast, in the silicon-rich NiSi melts the Ni diffusion coefficients are a factor 5 larger. In the figure are also included results from the MD simulations for the Ni diffusion

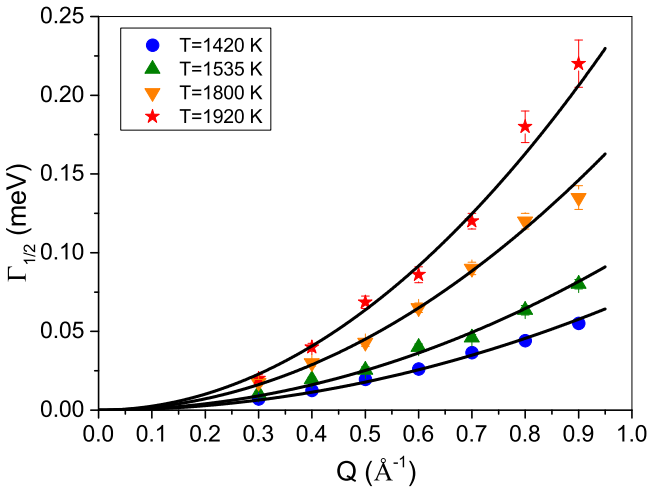

FIG. 3. The deduced HWHM from the Lorentzian fits are plotted. The lines depict a fit with $\Gamma_{1/2}(Q) = \hbar D Q^2$

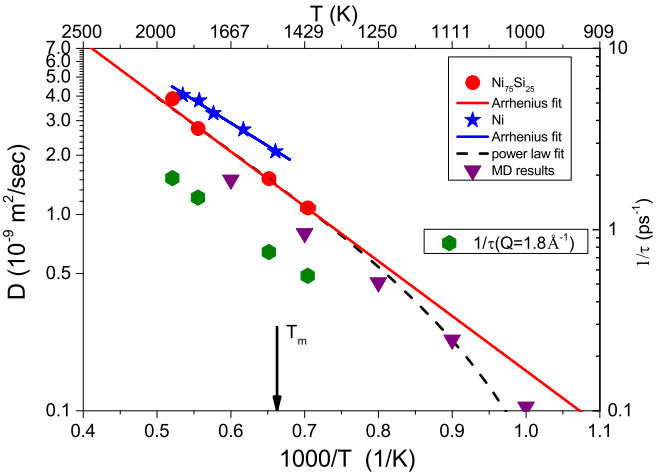

FIG. 4. The derived diffusion coefficients are plotted in comparison with values for liquid and supercooled pure Ni [12]. The error bars for the diffusion coefficients are smaller than the symbol size. The lines are Arrhenius law fits to the temperature dependence and the dashed line is a fit with a power law (see text for more details). Included are also values from the MD simulation for the nickel diffusion coefficients [8] and relaxation rates $1/\tau(Q = 1.8\,\text{Å}^{-1})$ (hexagons) from our data.

coefficient [8]. They are in general smaller, but the temperature dependence appears to be similar. The exact values depend at first on the density, which is in the simulation slightly smaller, and second, the potential might be a good but not perfect model for the real alloy. These simulation diffusion coefficients demonstrate that from around 1300 K the diffusion process starts to deviate from an Arrhenius law.

The temperature dependence of a diffusion process in a liquid can be described by an Arrhenius law: $D = D_0\exp(-\Delta E/k_B T)$ with k_B the Boltzmann constant, T the temperature, and ΔE the activation energy for the diffusion process. There is no theoretical basis for such a temperature dependence in a metallic liquid, but experimental diffusion coefficients of many liquid metals and alloys seem to follow an Arrhenius-type equation [30]. On a logarithmic scale that fit results in a linear dependence. The fit in Fig. 4 demonstrates that the temperature dependence of the diffusion process follows an Arrhenius behavior quite well even in the undercooled state and hence a diffusion process activated by a single activation energy is observed. A similar conclusion about the temperature dependence was achieved for liquid and undercooled Ni [12]. However, the activation energies are different. We obtain a $\Delta E = 556 \pm 40$ meV for $Ni_{75}Si_{25}$, whereas for liquid Ni $\Delta E = 470 \pm 30$ meV has been reported [12]. Here we observe a 10% larger activation energy compared to pure Ni. That increase in activation energy might be the reason for the reduced mobility compared to pure Ni. The increase in activation energy might be related to the nonideal mixing behavior of the NiSi melt, where with increasing Si concentration the molar volume decreases up to a Si concentration of about 30% [8]. The concomitant larger particle density might be the reason for the increasing activation energy and reduced mobility of the Ni ions. A structural investigation on a $Ni_{50}Si_{50}$ melt found evidence for remaining covalent bonding between silicon atoms [10], whereas at a higher Si concentration no evidence was reported. Included are relaxation rates $1/\tau(Q)$ derived at a larger momentum transfer $Q = 1.8\,\text{Å}^{-1}$. At that Q vector the quasielastic signal is composed of nickel self-diffusion and structural relaxation from the increasing coherent scattering contribution. The temperature dependence of that relaxation process is apparently very similar to the Arrhenius behavior of the self diffusion and does not indicate a separation in dynamics between self dynamics and correlated movements.

In the silicon-rich NiSi melts an activation energy of $\Delta E = 280 \pm 20$ meV was deduced [11] and the lower activation energy has been related to the factor 5 faster Ni self-diffusion in these compounds. The higher mobility of the Ni ions in the Si matrix might be understandable with the much more loose structure of fluid silicon, expressed in a larger molar volume [8] and reduced number of nearest neighbors [13] compared to liquid Ni. The structure of the silicon-rich melt can no more be described by a hard sphere fluid [9]. Liquid silicon shows an open-network-like structure with only six nearest neighbors [31], which is much less than the 12 nearest neighbors for a dense hard sphere liquid and already quite near to the tetrahedral coordination in solid silicon. In solid silicon a surprising large mobility of nickel was recently found [32], perhaps related to mobile interstitial Ni.

Wang *et al.* measured the surface tension in a liquid and undercooled Ni5%wtSi alloy. From these measurements viscosity and through the Stokes Einstein relation diffusion coefficients have been calculated [14]. The temperature dependence of D was described by an Arrhenius law from the 200 K undercooled state up to 400 K above the liquidus temperature. Nevertheless, it appears that toward the lower temperature the data points deviate from the Arrhenius fit.

Beyond these self-evident conclusions our data can be put into the wider context of the predictions from the MD simulations. The MD simulations of the $Ni_{75}Si_{25}$ composition predicted a power-law behavior up to about twice the glass temperature T_g, far above the melting temperature [15]. The structure does not change significantly from the liquid to the undercooled state; however, the dynamics changes dramatically toward the glass transition [33]. Mode coupling theory (MCT) of the liquid to glass transition is able to predict this slowing down on a quantitative basis [33]. Within this theory a critical temperature T_c is central for the dynamics, where structural relaxation is frozen out completely. A consequence is that toward the glass transition self-diffusion is described by a power-law behavior in contrast to an Arrhenius-law, expected for a thermally excited jump diffusion process [34]. The power-law has been found correct near T_c, however, MCT cannot forecast the range of temperatures over which such a prediction is quantitatively valid [34]. A power law has been observed in metallic glass formers, for example, in the Ni self-diffusion in a four-component metallic glass for temperatures around the liquidus temperature [35]. An exponent $\gamma = 2.7$ has been reported for the Ni diffusion in this system. Tracer diffusion measurements on the same compound for Co diffusion came to the same conclusion [36].

The MD simulation derived an exponent for the power-law for the Ni self-diffusion coefficients of $\gamma = 1.765$ and a $T_c = 703$ K [15]. We applied a fit with a power-law according to: $D = \text{const}(T - T_c)^{1.765}$. A fit with three free parameters for

four data points and the strong correlation between γ and T_c was not stable, hence we used the exponent from the simulation as a fixed parameter. That fit is included as a dashed line in Fig. 4 and is able to describe the data points as well as the Arrhenius law concerning the χ^2 value. We obtain a $T_c = 892 \pm 51$ K from the fit. Both temperature laws are compatible with the data and it is not possible to exclude one due to the limited temperature range. Clearly, deviations from the two different temperature dependencies should appear a few hundred Kelvin below our lowest measured temperature. The achieved undercooling of at most 100 K for several hours is not large enough to observe deviations from the Arrhenius behavior. From Fig. 1 we can deduce a maximum undercooling of about 250 K, which could be just near the temperature range when deviations might start to appear between the two laws. However, it is not clear for the moment how to achieve such a large undercooling for a reasonable long measurement time.

Still, it appears surprising that the power-law prediction from MCT can describe the diffusion coefficient and consequently further dynamical quantities, like structural relaxation time and viscosity, over such a large range of temperatures in a dense metallic melt. Götze reviewed and compared experimental results for glass formers with predictions of the MCT and found quantitative agreement in a temperature range of up to 20% above T_c [37]. That comparison was based on a number of profound predictions for structural relaxation. However, focusing on only one dynamic quantity an earlier assessment of experimental viscosity data of many liquids revealed a power-law behavior, which holds over a wide range of temperatures into the equilibrium liquid state [38]. Similarly, a MD-simulation on a Lennard-Jones binary liquid suggested a power law for the diffusion coefficient applicable far into the equilibrium liquid state [39]. At these high temperatures, the intermediate scattering function describing the tagged particle movements changed its shape from a Kohlrausch to an exponential decay, fully compatible with our fits and supporting our assumption for a power-law fit.

For metallic systems further MD simulations observed a change to a power-law behavior deep in the liquid state. For a glass forming $Cu_{33.3}Zr_{66.7}$ melt it has been demonstrated that both self-diffusion coefficients follow a power-law behavior with an exponent of $\gamma_{Cu} = 1.52$ and $\gamma_{Zr} = 1.93$ [40]. The power-law fit was applied successfully in a temperature range reaching several hundred degrees above the melting point. More recently a simulation on a CuZrAl alloy showed a dynamical crossover from an uncorrelated to a correlated state at a temperature within the equilibrium liquid state [41]. All these observations based on simulations suggest that within the liquid state there exists a change in dynamics evidenced by a change in character of the particle mobility toward solidification. The compatibility of our data with a power-law fit is, therefore, weight from the experimental point of view toward these simulation observations. The MD simulations on $Ni_{75}Si_{25}$ demonstrated for the product of self-diffusion and viscosity, hence quantities related to single particle and collective movements, a change in dynamics deep in the liquid state [15]. Our data on the self-diffusion of $Ni_{75}Si_{25}$ are compatible with the MD-simulation results and can be regarded as a first experimental hint for the supposed change in dynamics. Experimentally, a change in dynamics above the melting point has been observed in monatomic liquid metals monitoring the density fluctuations at the structure factor maximum, a quantity related to the decay of density correlations on next-neighbor distances and to a generalized viscosity [16–18]. That change was interpreted as a transition within the equilibrium liquid state toward a viscous, more solid-like state upon cooling. Further investigations revealed an additional slow relaxation process in the liquid dynamics [16], which previous MD simulations and theoretical considerations related to the onset of structural freezing toward solidification [42]. One might conclude that the observed compatibility of our data with the power law for the self-diffusion is evidence for the change in dynamics in $Ni_{75}Si_{25}$ toward solidification. Further experimental efforts are necessary to put more weight on this assumption.

IV. CONCLUSIONS

A quasielastic neutron-scattering experiment on $Ni_{75}Si_{25}$ has been performed in the liquid and undercooled state. To this end an aerodynamic levitation setup was installed on the neutron spectrometer where a small sphere of 2.7-mm diameter was heated by two CO_2 lasers. An undercooling of 90 K for several hours was achieved. The dominating scattering contribution at small wave vectors stems from the self-diffusion of nickel. The derived diffusion coefficients for Ni are similar to pure Ni and the temperature dependence can be described by an Arrhenius law. The activation energy is about 10% larger compared to pure liquid Ni, which might be related to a change in interaction energy with the addition of silicon. MD-simulations showed a departure from an Arrhenius behavior toward a power-law temperature dependence for the Ni self-diffusion in $Ni_{75}Si_{25}$ at a temperature of about twice T_g. Our data are compatible with such a power law, which has a theoretical foundation in the mode-coupling theory for the glass transition. From the limited data set we are not able to differentiate between Arrhenius and power-law behavior and a much larger undercooling would be necessary to observe the expected differences in the temperature behavior. Furthermore, a viscosity measurement over a wide temperature range would be an important transport parameter to characterize the collective movement of the particles and hence to support the suggestion that the dynamics changes within the equilibrium liquid state in $Ni_{75}Si_{25}$.

ACKNOWLEDGMENTS

We thank the ILL for provision of beamtime and the IN6 staff for help with the experiment. Part of this work was supported by the Science and Technology Facilities Council, STFC.

[1] P. G. Debenedetti and F. H. Stillinger, Nature **410**, 259 (2001).
[2] A. L. Greer, Nat. Mater. **14**, 542 (2015).
[3] Y. Wu, J. Xiang, C. Yang, W. Lu, and C. H. Lieber, Nature **430**, 61 (2004).

[4] A. Wagner, B. A. Shollock, and M. McLean, Mater. Sci. Eng. A **374**, 270 (2004); R. F. Cochrane, A. L. Greer, K. Eckler, and D. M. Herlach, *ibid.* **133**, 698 (1991).

[5] Y. Lu, G. Yang, F. Liu, H. Wang, and Y. Zhou, Europhys. Lett. **74**, 281 (2006).

[6] D. Connetable and O. Thomas, J. Alloys Comp. **509**, 2639 (2011).

[7] M. Leonhardt, W. Löser, and H. G. Lindenkreuz, Mater. Sci. Eng. A **271**, 31 (1999).

[8] Y. J. Lu and P. Entel, Phys. Rev. B **84**, 104203 (2011).

[9] Y. Waseda and S. Tamaki, Philos. Mag. B **32**, 951 (1975).

[10] S. Gruner, J. Marczinke, L. Hennet, W. Hoyer, and G. J. Cuello, J. Phys.: Condens. Matter **21**, 385403 (2009).

[11] A. I. Pommrich, A. Meyer, D. Holland-Moritz, and T. Unruh, Appl. Phys. Lett. **92**, 241922 (2008).

[12] A. Meyer, S. Stüber, D. Holland-Moritz, O. Heinen, and T. Unruh, Phys. Rev. B **77**, 092201 (2008).

[13] H. Kimura, M. Watanabe, K. Izumi, T. Hibiya, D. Holland-Moritz, T. Schenk, K. R. Bauchspiess, S. Schneider, K. Funakoshi, and M. Hanfland, Appl. Phys. Lett. **78**, 604 (2001).

[14] H. P. Wang, C. D. Cao, and B. Wei, Appl. Phys. Lett. **84**, 4062 (2004).

[15] Y. J. Lu, H. Cheng, and M. Chen, J. Chem. Phys. **136**, 214505 (2012).

[16] F. Demmel, A. Diepold, H. Aschauer, and C. Morkel, Phys. Rev. B **73**, 104207 (2006); F. Demmel, P. Fouquet, W. Häussler, and C. Morkel, Phys. Rev. E **73**, 032202 (2006); F. Demmel and C. Morkel, *ibid.* **85**, 051204 (2012).

[17] F. Demmel, W. S. Howells, and C. Morkel, J. Phys.: Condens. Matter **20**, 205106 (2008); F. Demmel, W. S. Howells, C. Morkel, and W. C. Pilgrim, Z. Phys. Chem. **224**, 83 (2010).

[18] F. Demmel, A. Fraile, D. Szubrin, W. C. Pilgrim, and C. Morkel, J. Phys.: Condens. Matter **27**, 455102 (2015).

[19] C. Landron, L. Hennet, T. E. Jenkins, G. N. Greaves, J. P. Coutures, and A. K. Soper, Phys. Rev. Lett. **86**, 4839 (2001).

[20] H. Sinn, B. Glorieux, L. Hennet, A. Alatas, M. Hu, E. E. Alp, F. J. Bermejo, D. L. Price, and M. L. Saboungi, Science **299**, 2047 (2003).

[21] L. Hennet, I. Pozdnyakova, A. Bytchkov, V. Cristiglio, P. Palleau, H. E. Fischer, G. J. Cuello, M. Johnson, P. Melin, D. Zanghi, S. Brassamin, J.-F. Brun, D. L. Price, and M. L. Saboungi, Rev. Sci. Instrum. **77**, 053903 (2006).

[22] C. Landron, L. Hennet, J. P. Coutures, T. Jenkins, C. Aletru, G. N. Greaves, A. K. Soper, and G. Derbyshire, Rev. Sci. Instrum. **71**, 1745 (2000).

[23] J. Kozaily, L. Hennet, H. Fischer, M. Koza, S. Brassamin, S. Magazu, and F. Kargl, Phys. Status Solidi C **8**, 3155 (2011).

[24] V. F. Sears, Neutron News **3**, 26 (1992).

[25] T. Schenk, D. Holland-Moritz, V. Simonet, R. Bellissent, and D. M. Herlach, Phys. Rev. Lett. **89**, 075507 (2002).

[26] Y. Waseda, *The Structure of Non-Crystalline Materials* (McGraw Hill, New York, 1980).

[27] F. Demmel, L. Hennet, M. Koza, J. Kozaily, and D. R. Neuville, *Dynamics and Fragility of the Metallic Alloy NiSi*, Institut Laue-Langevin (ILL, Grenoble, 2013), doi:10.5291/ILL-DATA.6-03-425.

[28] http://www.ill.eu/instruments-support/computing-for-science/cs-software/all-software/lamp/

[29] J. P. Hansen and I. R. McDonald, *Theory of Simple Liquids* (Academic Press, London, 2006).

[30] T. Ida and R. I. L. Guthrie, *The Thermophysical Properties of Metallic Liquids* (Oxford University Press, Oxford, 2015).

[31] T. H. Kim, G. W. Lee, B. Sieve, A. K. Gangopadhyay, R. W. Hyers, T. J. Rathz, J. R. Rogers, D. S. Robinson, K. F. Kelton, and A. I. Goldman, Phys. Rev. Lett. **95**, 085501 (2005); S. Ansell *et al.*, J. Phys.: Condens. Matter **10**, L73 (1998).

[32] J. Lindross, D. P. Fenning, D. J. Backlund, E. Verlage, A. Gorgulla, S. K. Estreicher, H. Savin, and T. Buonassisi, J. Appl. Phys. **113**, 204906 (2013).

[33] W. Götze, *Complex Dynamics of Glass-forming Liquids* (Oxford University Press, Oxford, 2009).

[34] W. Kob, Supercooled Liquids, the Glass Transition and Computer Simulations, arXiv:cond-mat/0212344.

[35] A. Meyer, Phys. Rev. B **66**, 134205 (2002).

[36] V. Zöllmer, K. Rätzke, F. Faupel, and A. Meyer, Phys. Rev. Lett. **90**, 195502 (2003).

[37] W. Götze, J. Phys.: Condens. Matter **11**, A1 (1999).

[38] P. Taborek, R. N. Kleiman, and D. J. Bishop, Phys. Rev. B **34**, 1835 (1986).

[39] S. Kämmerer, W. Kob, and R. Schilling, Phys. Rev. E **58**, 2131 (1998).

[40] X. J. Han and H. R. Schober, Phys. Rev. B **83**, 224201 (2011).

[41] A. Jaiswal, T. Egami, and Y. Zhang, Phys. Rev. B **91**, 134204 (2015).

[42] U. Balucani and R. Vallauri, Phys. Rev. A **40**, 2796 (1989).